21st European Conference on Fracture, ECF21, 20-24 June 2016, Catania, Italy

On constitutive assumptions in phase field approaches to brittle fracture

Michael Strobl[a], Thomas Seelig[a]

[a]*Institute of Mechanics, Karlsruhe Institute of Technology, Otto-Ammann-Platz 9, 76131 Karlsruhe, Germany*

Abstract

Constitutive assumptions involved in phase field models of fracture in order to capture the behavior of cracks on the (smeared) continuum level are critically reviewed and several improvements are suggested. While some of the deficiencies of existing models are connected to the variational structure of respective phase field approaches, non-variational approaches are shown to allow for greater flexibility towards constitutive assumptions needed for a realistic representation of cracks. Benefits of the latter are illustrated by numerical examples.

Keywords: Brittle fracture; Phase field approach; Finite elements; Crack nucleation; Damage mechanics

1. Introduction

Phase field approaches to brittle fracture have recently proven their excellent ability to reproduce situations with complex crack patterns including initiation of cracks and determination of unknown crack paths, e.g. Karma et al. (2001), Henry and Levine (2004), Miehe et al. (2010a) and Kuhn and Müller (2010). These features follow directly from variational global energy minimization principles extending the classical Griffith theory of fracture as suggested by Francfort and Marigo (1998) and cast into a regularized (phase field) approximation by Bourdin et al. (2000), which is more suitable for a numerical (e.g. finite element) solution. In certain cases, however, additional constitutive assumptions have to be included in the phase field model in order to obtain physically reasonable solutions. For instance, these assumptions aim to prevent damage in compressed regions by introducing a tension-compression asymmetric material response (e.g. Amor et al. (2009)) or prevent the onset of damage before a critical state is reached (e.g. Miehe et al. (2015)). To some extent, this can only be achieved at the cost of giving up the underlying variational concept of brittle fracture.

The present work focuses on the choice of constitutive assumptions and analyzes their impact on the perfor-

---

* Corresponding author. Tel.: +49 721 608 47794 ; fax: +49 721 608 47990.
  E-mail address: michael.strobl@kit.edu

10.1016/j.prostr.2016.06.460

Fig. 1. Elastic body with (a) a sharp crack $\Gamma \subset R^{ndm-1}$ and (b) a phase field approximation $s(x)$ of the crack by a smooth transition between $s = 1$ for intact material far away from the crack and $s = 0$ for the fully broken state of material in the crack.

mance of phase field models for brittle fracture. These constitutive assumptions concern, firstly, the proper representation of crack "boundary" conditions and, secondly, the evolution equation for the phase field. Since in variationally consistent approaches these two aspects are too strongly tied to each other, different formulations of non-variationally derived but physically motivated phase field evolution laws are discussed, primary based on energetic concepts. In Sect. 2 the fundamental equations of the phase field approach to dynamic brittle fracture are presented. A detailed discussion of different constitutive assumptions and their consequences in the phase field modeling of cracks is provided for variationally consistent approaches in Sect. 3 and for non-variational extensions in Sect. 4. Some numerical examples are presented in Sect. 5 and conclusions are drawn in Sect. 6.

2. A continuum phase field approach for brittle fracture

In order to regularize the sharp surface of a crack and the corresponding strong discontinuity in the displacement field an additional scalar field s is introduced. This field continuously varies between the undamaged material $s = 1$ and the fully broken state of material $s = 0$, see Fig. 1. With Griffith's critical energy release rate $\mathcal{G}_c$ this enables to approximate the surface energy

$$\int_\Gamma \mathcal{G}_c \, dA_s \approx \int_\Omega \mathcal{G}_c \, \gamma_\ell(s) \, dV \tag{1}$$

by a surface energy density $\gamma_\ell(s)$ which is defined in the whole domain Ω. The regularized crack surface density γ_ℓ is typically represented as

$$\gamma_\ell(s, \nabla s) = \frac{(1-s)^2}{2\ell} + \frac{\ell}{2} |\nabla s|^2 \tag{2}$$

which includes the spatial gradient of the phase field, see e.g. Bourdin et al. (2000). The transition zone between undamaged and broken states is controlled by the length parameter $\ell > 0$. Neglecting volume forces, the total free energy E of a cracked body can be written as

$$E(\boldsymbol{u}, s) = \int_\Omega \psi(\boldsymbol{u}, s) \, dV = \int_\Omega \psi_{el}(\boldsymbol{u}, s) \, dV + \int_\Omega \mathcal{G}_c \, \gamma_\ell(s) \, dV \tag{3}$$

where the elastic portion depends on the displacement $\boldsymbol{u}$ through the infinitesimal strain tensor $\boldsymbol{\varepsilon} = (\nabla \boldsymbol{u} + \nabla^{\mathrm{T}} \boldsymbol{u})/2$.

2.1. Variational framework and FEM implementation

Using Hamilton's principle the strong form of the momentum balance and phase field evolution equation may be derived, see e.g. Borden et al. (2012), Hofacker and Miehe (2012), Schlüter et al. (2014), as

$$\rho \, \ddot{\boldsymbol{u}} - \mathrm{div} \, \boldsymbol{\sigma} = \boldsymbol{0}, \qquad \frac{\partial \psi_{el}}{\partial s} + \mathcal{G}_c \left(\frac{s-1}{\ell} - \ell \, \Delta s \right) = 0 \tag{4}$$

with the Laplacian Δs of the phase field. The corresponding mechanical and phase field boundary conditions are

$$\boldsymbol{u} = \bar{\boldsymbol{u}} \text{ on } \partial\Omega_u, \qquad \boldsymbol{\sigma} \cdot \boldsymbol{n} = \bar{\boldsymbol{t}} \text{ on } \partial\Omega_t, \qquad \nabla s \cdot \boldsymbol{n} = 0 \text{ on } \partial\Omega \tag{5}$$

with $\partial\Omega = \partial\Omega_t \cup \partial\Omega_u$, $\partial\Omega_t \cap \partial\Omega_u = \emptyset$ and the unit normal vector $\boldsymbol{n}$. In general, only some part of the stored bulk energy is influenced by the phase field, which is typically described by a scalar degradation function $g(s)$. Therefore the energy of an undamaged elastic solid $\psi_{0\,el} = (\boldsymbol{\varepsilon} : \mathbb{C}_0 : \boldsymbol{\varepsilon})/2 = \psi_{0\,act} + \psi_{0\,pas}$ is decomposed into an active part and a passive part as entitled in Murakami (2012). The specific choice of the split

$$\psi_{el}(\boldsymbol{\varepsilon}, s) = g(s)\,\psi_{0\,act}(\boldsymbol{\varepsilon}) + \psi_{0\,pas}(\boldsymbol{\varepsilon}) \tag{6}$$

is discussed in Sect. 3 and Sect. 4. Including this additive split of energies, the evolution equation (4_2) reads

$$g'(s)\,\overbrace{\psi_{0\,act}(\boldsymbol{\varepsilon})}^{D_s} - \underbrace{\mathcal{G}_c\left(\frac{1-s}{\ell} + \ell\,\Delta s\right)}_{\text{crack resistance } R_s} = 0 \tag{7}$$

$$\underbrace{\phantom{g'(s)\,\psi_{0\,act}(\boldsymbol{\varepsilon})}}_{\text{crack driving force}}$$

with $g'(s) = \mathrm{d}\,g/\mathrm{d}s$. So the scalar valued crack driving force on the left hand side, including the energetic expression D_s, and the crack resistance R_s on the right are in equilibrium.

In order to solve the coupled set of PDEs we obtain a standard finite element implementation with a monolithic or staggered solution scheme.

2.2. Irreversibility of phase field evolution

Due to the choice of the monotonous function γ_ℓ for the description of the crack surface, see Eq. (2), it is necessary to introduce an irreversibility condition to prevent crack healing. This can be accomplished, for instance, by imposing a Dirichlet type boundary condition where the material is close to the fully damaged state

$$s(\boldsymbol{x}, t > t_o) \overset{!}{=} 0 \qquad \text{if} \qquad s(\boldsymbol{x}, t_o) \approx 0. \tag{8}$$

Alternatively, one may enforce a non-negative damage rate $\dot{s} \leq 0$. This is e.g. realized by the introduction of a damage-driving strain energy history parameter $\mathcal{H}$, which ensures the Clausius-Duhem inequality and adds a local irreversibility constraint, see Miehe et al. (2010b) for more details.

2.3. Pre-existing cracks

Closely related to the irreversibility of the phase field is the question of how to set crack boundary conditions in case of pre-existing cracks. Of course, initial cracks can be modeled as discrete cracks using double nodes in the finite element mesh. However, in the present work all, i.e. pre-existing and evolving, cracks are modeled by the phase field and the impact of constitutive relations on their behavior (including contact by crack closure) is investigated. One possibility is to constrain the phase field by prescribing Dirichlet boundary conditions $s(\boldsymbol{x}_\Gamma, t = 0) \overset{!}{=} 0$ at the crack. The constrained nodes can lie on a single line or on a broader region. The latter option leads to a small remaining stiffness and is therefore favored, but results in significantly larger errors in terms of the crack surface energy, see
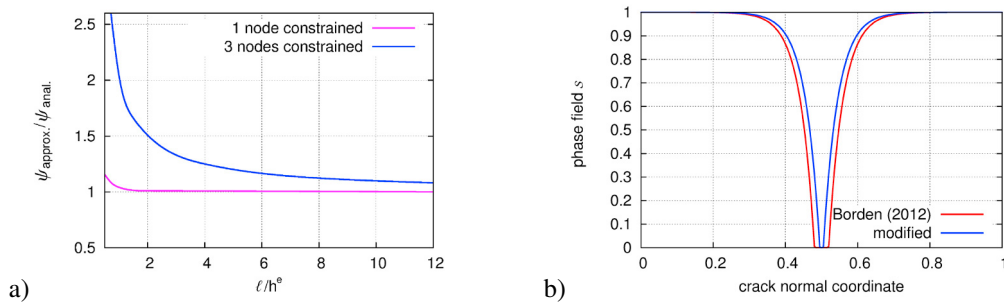

Fig. 2. Effect of smeared crack modeling: (a) accuracy of the approximated surface energy for one and three constrained nodes over the thickness of the crack, depending on the ratio ℓ/h^e; (b) profile of the phase field with an initial crack induced by a prescribed history field $\mathcal{H}(\boldsymbol{x}, t = 0)$, comparison of the original formulation and the here used modified version for $h^e = \ell/4$.

Fig. 2(a). This finding can also be transferred to evolving cracks, which dissipate for small ratios ℓ/h^{e} significantly more energy than in the continuous prediction. Alternatively, if the aforementioned history field is used an initial crack can be induced by prescribing initial history values, see Borden et al. (2012). Another benefit is that the crack can be set independent of the mesh. However, we modify the original formulation by limiting the range of the initial energy distribution to the element size h^{e}. This reduces for $\ell > 2h^{\mathrm{e}}$ the width of the fully damaged zone significantly as can be seen in Fig. 2(b). The initial value can be computed by

$$\mathcal{H}(\boldsymbol{x}, t_0) = \frac{\mathcal{G}_{\mathrm{c}}\,(1 - s_0)}{2\ell\,s_0}\,\frac{\langle h^{\mathrm{e}} - d(\boldsymbol{x}, l_{\mathrm{cs}})\rangle}{h^{\mathrm{e}}} \tag{9}$$

with the function $\langle x \rangle = (|x| + x)/2$, the initial phase field value $s_0 = s(\boldsymbol{x}, t = 0) \ll 1$ at the crack and the closest distance d to the crack surface l_{cs}.

2.4. Degradation function

The degradation function $g(s)$, introduced in Eq. (6), describes the release of stored bulk energy and reduction of stiffness. Therefore it should be monotonously decreasing from $g(1) = 1$ in the undamaged to $g(0) = 0$ in the fully broken state. Its first derivative $g'(s) = \mathrm{d}\,g/\,\mathrm{d}s$ controls the contribution of the bulk energy in the phase field evolution equation with $g'(0) = 0$. A simple choice for the function fulfilling all these properties and will be used for the numerical examples in Sect. 5 is the quadratic function $g = s^2 + k$. The small additional parameter $k \approx 0$ guarantees the well-posedness of the model in case of full degradation. The onset of stiffness reduction and the point of failure can be influenced to some extent by the choice of the function $g(s)$ as discussed by Kuhn et al. (2015).

3. Constitutive modeling – variationally consistent methods

The aforementioned introduced phase field approach for fracture, based on the Helmholtz free energy function in Eq. (3), relies on some constitutive assumptions. In detail, the choice of the aforementioned degradation function $g(s)$ as well as the composition of the elastic energy $\psi_{\mathrm{el}}(\boldsymbol{u}, s)$ is up to the model. This section provides a discussion of these and other constitutive assumptions, closely related to the context of damage mechanics and motivated by experimental findings. First phase field models for fracture, e.g. in Karma et al. (2001), Bourdin et al. (2008) or Kuhn and Müller (2010), assumed that the whole stored bulk energy undergoes degradation

$$\psi_{\mathrm{el}}(\boldsymbol{u}, s) = g(s)\,\psi_{0\,\mathrm{el}}, \tag{10}$$

with $\psi_{0\,\mathrm{el}}$ being the energy of the undamaged elastic solid. This may lead cracking in compressed regions. In order to overcome this unphysical feature the elastic energy is additively split into "active" and "passive" parts where only the latter is degraded by the phase field as shown in Eq. (6) and thus appears in the evolution equation (7). The different treatment of the energetic parts breaks the symmetry of tension and compression. While the split of a scalar strain or stress and the corresponding elastic energy is clear, in two or three dimensions the split of a second order tensor is not unique and demands constitutive definitions. Two approaches are so far well established and shortly introduced in a uniform notation here.

3.1. Volumetric-deviatoric split

Amor et al. (2009) introduced the so called unilateral contact model in the context of phase field modeling. The formulation is based on the split into volumetric and deviatoric parts of the strain. It is motivated by the assumption that material expansion, including opening of cracks, takes place where the sign of the local volume change, the trace of the strain tensor $\varepsilon_{\mathrm{V}} = \mathrm{tr}\,(\boldsymbol{\varepsilon})$, is positive. Thus only the stiffness related to the positive volumetric and the deviatoric part $\boldsymbol{\varepsilon}_{\mathrm{D}} = \boldsymbol{\varepsilon} - \varepsilon_{\mathrm{V}}\mathbf{1}$ are degraded by the phase field. The corresponding active part of the elastic energy and Cauchy stress tensor are

$$\psi_{0\,\mathrm{act}} = \frac{K}{2}\,\langle \mathrm{tr}\,(\boldsymbol{\varepsilon})\rangle^2 + \mu\,(\boldsymbol{\varepsilon}_{\mathrm{D}} : \boldsymbol{\varepsilon}_{\mathrm{D}}), \qquad \boldsymbol{\sigma} = \frac{\partial \psi_{\mathrm{el}}}{\partial \boldsymbol{\varepsilon}} = g(s)\left(K\,\langle \mathrm{tr}\,(\boldsymbol{\varepsilon})\rangle\,\mathbf{1} + 2\mu\,\boldsymbol{\varepsilon}_{\mathrm{D}}\right) - K\,\langle -\,\mathrm{tr}\,(\boldsymbol{\varepsilon})\rangle\,\mathbf{1}, \tag{11}$$

where K and μ denote the bulk and shear modulus respectively. The negative volumetric part remains unaffected by the phase field in order to establish a non-interpenetration condition where the material is compressed. In both cases, for an open and closed crack, the constitutive material behavior remains isotropic

$$\mathbb{C}_{\text{act}} = g(s)\left(\lambda\,\mathbf{1}\otimes\mathbf{1} + 2\mu\,\mathbb{I}\right), \qquad\qquad \mathbb{C}_{\text{pas}} = \left(\lambda + \frac{2}{3}\mu\left(1 - g(s)\right)\right)\mathbf{1}\otimes\mathbf{1} + 2g(s)\mu\,\mathbb{I}. \tag{12}$$

The crack driving force is derived by consistent variation

$$D_s = \psi_{0\,\text{act}} = \frac{K}{2}\langle\text{tr}(\boldsymbol{\varepsilon})\rangle^2 + \mu\,(\boldsymbol{\varepsilon}_{\text{D}} : \boldsymbol{\varepsilon}_{\text{D}}). \tag{13}$$

Only positive volume changes and distortion of the shape activate crack driving forces.

3.2. Spectral decomposition

The second model is based on the spectral decomposition of strains and supposes that the crack opening and growth is induced by the positive principal strains

$$\boldsymbol{\varepsilon}_+ = \sum_{i=1}^{3} \langle\varepsilon_i\rangle\, \boldsymbol{n}_i \otimes \boldsymbol{n}_i = \boldsymbol{Q}_+\,\boldsymbol{\varepsilon}\,\boldsymbol{Q}_+^{\text{T}} \qquad \text{with} \qquad \boldsymbol{Q}_+ = \sum_{i=1}^{3} H(\varepsilon_i)\,\boldsymbol{e}_i \otimes \boldsymbol{n}_i. \tag{14}$$

For this purpose, the positive projection tensor $\boldsymbol{Q}_+$ according to Lubarda et al. (1994) is used, with the principal strains ε_i and principal strain directions $\boldsymbol{n}_i$. In the context of the phase field approach to fracture, the split has been introduced by Miehe et al. (2010a). The active part of the elastic energy and the Cauchy stress read

$$\psi_{0\,\text{act}} = \frac{\lambda}{2}\langle\text{tr}(\boldsymbol{\varepsilon})\rangle^2 + \mu\,\text{tr}(\boldsymbol{\varepsilon}_+)^2, \qquad \boldsymbol{\sigma} = g(s)\left(\lambda\,\langle\text{tr}(\boldsymbol{\varepsilon})\rangle\,\mathbf{1} + 2\mu\,\boldsymbol{\varepsilon}_+\right) - \left(\lambda\,\langle-\text{tr}(\boldsymbol{\varepsilon})\rangle\,\mathbf{1} - 2\mu\,(\boldsymbol{\varepsilon} - \boldsymbol{\varepsilon}_+)\right) \tag{15}$$

and include the volumetric strain and the principle strains as long as they are positive. Unless all principal strains are either positive or negative the material behavior under damage is transversely isotropic oriented with the loading direction. The local crack driving force occuring in the variational consistent evolution equation reads

$$D_s = \frac{\lambda}{2}\langle\text{tr}(\boldsymbol{\varepsilon})\rangle^2 + \mu\,\text{tr}(\boldsymbol{\varepsilon}_+)^2. \tag{16}$$

4. Constitutive assumptions – variationally non-consistent approaches

Both splits (volumetric-deviatoric and spectral decomposition) in the way they are used above fully preserve the variational character of the method. Then the choice of the energetic split controls the energy contribution in the damage evolution as well as the non-interpenetration condition. This is rather restrictive regarding the incorporation of different damage and failure criteria. In addition, the state of fully degraded material ($s \ll 1$) should reproduce the behavior of a macroscopic crack, at least in a regularized sense. This means that the normal stress on the crack should be non-positive and the shear stresses along a frictionless crack should vanish. By giving up the variational structure of the phase field model, the stress response and the crack driving force in the phase field evolution equation (4_2) can be adapted independently.

4.1. Crack boundary conditions including contact

The asymmetric tension-compression response of $\boldsymbol{\sigma}$ representing a crack in a "smeared" sense in the phase field approach should prevent material interpenetration and enable the transfer of compressive stresses across the crack. This results in a transversely isotropic material behavior oriented with the crack normal in the damaged crack region. The crack orientation, i.e. its unit normal vector, can be computed from the gradient of the phase field: $\boldsymbol{n}_s = -\nabla s/|\nabla s|$. Crack opening or closure is in the present (damage-like) continuous crack representation determined by the crack normal strain $\varepsilon_{nn} = \boldsymbol{n}_s \cdot \boldsymbol{\varepsilon} \cdot \boldsymbol{n}_s \gtrless 0$. In the following two constitutive models based on a *crack orientation dependent*

decomposition of $\boldsymbol{\sigma}$ in portions affected ("active") and unaffected ("passive") by the phase field are presented where for simplicty a frictionless crack face contact is assumed.

4.1.1. Simple unilateral normal contact

The first model determines crack opening by checking the sign of the crack normal strain ε_{nn}. In case of $\varepsilon_{nn} > 0$ all stress components are degraded

$$\boldsymbol{\sigma}_{\text{act}} = g(s)\left(\lambda\, \text{tr}(\boldsymbol{\varepsilon})\,\mathbf{1} + 2\mu\,\boldsymbol{\varepsilon}\right) \tag{17}$$

in order to guarantee a traction-free surface. In contrast, a negative normal strain $\varepsilon_{nn} < 0$ leads to an elastic stress response in the crack normal direction with

$$\boldsymbol{\sigma}_{\text{pas}} = g(s)\,\lambda\, \text{tr}(\boldsymbol{\varepsilon})\,\mathbf{1} + 2g(s)\mu\,\boldsymbol{\varepsilon} + (1 - g(s))(\lambda + 2\mu)\left(\boldsymbol{\varepsilon} : \boldsymbol{N}\right)\boldsymbol{N} \qquad \text{where} \qquad \boldsymbol{N} = \boldsymbol{n}_s \otimes \boldsymbol{n}_s \tag{18}$$

and displays a transversely isotropic material behavior oriented with the crack normal. Note that the stiffness parallel to the crack is reduced in both cases.

4.1.2. Physically consistent crack orientation dependent degradation

In a more sophisticated approach, see Strobl and Seelig (2015), only the stiffness normal to the crack is degraded. Crack opening is determined by a positive normal stress $\sigma_{nn}^{\text{trial}} = \boldsymbol{N} : \mathbb{C}_0 : \boldsymbol{\varepsilon}$. Tensile and shear stresses on the crack surfaces should vanish in the fully developed crack. Despite the scalar phase field parameter an open crack influences the normal stresses parallel to the crack in a physically correct anisotropic manner. These properties are computed by

$$\boldsymbol{\sigma}_{\text{act}} = \left(\lambda + (g(s) - 1)\frac{\lambda^2}{\lambda + 2\mu}\right)\text{tr}(\boldsymbol{\varepsilon})\,\mathbf{1} + 2\mu\,\boldsymbol{\varepsilon} + (g(s) - 1)\left(\lambda + \frac{\lambda^2}{\lambda + 2\mu}\right)\left(\text{tr}(\boldsymbol{\varepsilon})\,\boldsymbol{N} + (\boldsymbol{\varepsilon} : \boldsymbol{N})\,\mathbf{1}\right)$$
$$+ 4\,(1 - g(s))\left(\lambda + 2\mu - \frac{\lambda^2}{\lambda + 2\mu}\right)(\boldsymbol{\varepsilon} : \boldsymbol{N})\,\boldsymbol{N} + \mu\,(g(s) - 1)\left(\boldsymbol{N} \cdot \boldsymbol{\varepsilon} + \boldsymbol{\varepsilon} \cdot \boldsymbol{N}\right). \tag{19}$$

In case of compression only shear stresses parallel to the crack are degraded. The corresponding stress tensor reads

$$\boldsymbol{\sigma}_{\text{pas}} = \lambda\, \text{tr}(\boldsymbol{\varepsilon})\,\mathbf{1} + 2\mu\,\boldsymbol{\varepsilon} + 4\mu\,(1 - g(s))(\boldsymbol{\varepsilon} : \boldsymbol{N})\,\boldsymbol{N} + \mu\,(g(s) - 1)\left(\boldsymbol{N} \cdot \boldsymbol{\varepsilon} + \boldsymbol{\varepsilon} \cdot \boldsymbol{N}\right). \tag{20}$$

The corresponding stiffness tensor displays transverse isotropy with symmetry about the crack normal. It is described by only two material parameters (λ, μ) and the phase field s.

4.2. Phase field evolution equation

In addition to an appropriate stress response a constitutive model for the phase field evolution equation (7) is needed, where the crack driving force D_s plays the key role. A generale framework to formulate phase field evolution laws is proposed by Miehe et al. (2015). By using the strain energy history to assure local irreversibility (Sect. 2.2) the crack driving force D_s is replaced by its maximum value obtained in history:

$$\mathcal{H}(\boldsymbol{x}, t) = \max_{\tau \in [0,t]}\left(D_s(\boldsymbol{\varepsilon}(\boldsymbol{x}, \tau))\right). \tag{21}$$

4.2.1. Damage threshold

Brittle materials tend to fail with almost no preceding loss of stiffness. However, the classical strain energy based damage formulation leads to a significant degradation already at low stress levels. Hence the onset of damage should be controlled by a threshold. This can be easily accomplished by introducing a critical strain energy value ψ_c allowing a phase field evolution only if this value is exceeded, e.g. Karma et al. (2001):

$$D_s = \langle \psi(\boldsymbol{\varepsilon}) - \psi_c \rangle. \tag{22}$$

4.2.2. Stress based criteria

From an engineering point of view and in particular for brittle materials it is more suitable to deal with critical stress states. Moreover, in the aforementioned strain energy based criterion the critical stress for failure depends on the
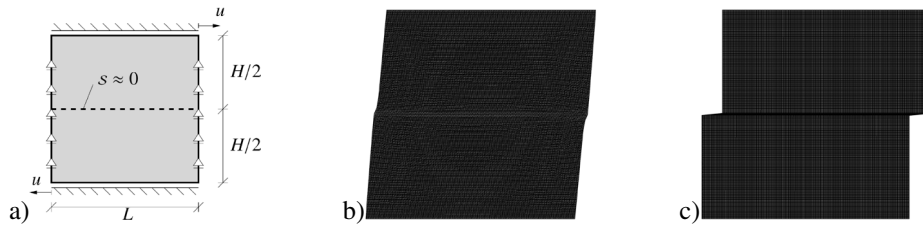
Fig. 3. Block with initial through-crack under shear loading (a) problem setup, (b) deformed mesh (100x exaggerated) using spectral decomposition, (c) deformed mesh (100x exaggerated) using a crack orientation dependent degradation.

length parameter ℓ, see Borden et al. (2012) and Kuhn and Müller (2013). Criteria based directly on a uniaxial failure stress σ_c may be formulated, here using the quadratic degradation function $g(s) = s^2 + k$, as

$$D_s = \frac{\zeta \, \mathcal{G}_c}{2\ell} \left\langle \sum_{i=1}^{3} \left(\frac{\langle \tilde{\sigma}_i \rangle}{\sigma_c} \right)^2 - 1 \right\rangle \qquad \text{or} \qquad D_s = \frac{\zeta \, \mathcal{G}_c}{2\ell} \left\langle \frac{1}{\sigma_c^2} \max \left(\langle \tilde{\sigma}_1 \rangle^2, \langle \tilde{\sigma}_2 \rangle^2, \langle \tilde{\sigma}_3 \rangle^2 \right) - 1 \right\rangle \qquad (23)$$

in terms of the sum of the effective principal tensile stresses $\tilde{\sigma}_i = \sigma_i / g(s)$ or the first effective principal tensile stress, respectively. The scalar factor $\frac{1}{2} \zeta \, \mathcal{G}_c / \ell$ with $\zeta > 0$ eliminates the influence of the length parameter ℓ from the evolution equation and controls the driving force after the onset of damage.

5. Numerical examples

This section demonstrates the different effects of the ingredients of the phase field approach discussed above. Giving up the variational structure leads to a higher numerical effort due to an unsymmetric tangent operator. This can be overcome by using a staggered solution scheme which involves only symmetric matrices. However, in order to obtain accurate results, especially in case of crack initiation, the usage of an appropriate stopping criterion in the staggered cycle following Ambati et al. (2014) is suggested. The following examples consider plane strain and use reasonable material parameters.

5.1. Testing of crack boundary conditions

In order to show the necessity of taking the crack normal $\boldsymbol{n}_s$ into account (Sect. 4.1), a simple numerical test of a loaded elastic through-cracked block is performed. Results of the compressed block can be looked up in Strobl and Seelig (2015). In contrast to the spectral decomposition and the volumetric-deviatoric split, which show significant problems to reproduce the homogeneous stress response, the results using the crack orientation dependent degradation of Sect. 4.1.2 are in perfect agreement with the analytical solution. The simple unilateral normal contact suffers from the stiffness degradation in the crack parallel direction. However, this error seems to be acceptable for the small Poisson's ratios of brittle materials. In case of shear (Fig. 3(a)) we do expect a large relative displacement at the crack with no elastic response. Despite a completely reduced phase field, the spectral decomposition shows a stiff response (Fig. 3(b)) which actually causes further unphysical fracture under increased loading. In contrast, formulations taking the crack normal into account show the expected response as shown in terms of the deformed mesh in Fig. 3(c).

5.2. Plate subjected to shear load

We now investigate a rectangular plate with an initial crack subjected to a horizontal displacement, see Fig. 4(a), in order to qualitatively analyze crack evolution. The initial crack is modeled by applying initial history values with $s_0 = 0.01$. In addition, to capture the crack behavior accurately the mesh in areas close to the existing crack and expected crack propagation zone is refined. With the exception of the spectral decomposition, which leads to a quite stiff response and unphysical crack evolution due to the problems mentioned in the aforegoing example, other formulations taking a tension-compression split into account reproduce a single evolving crack as shown in Fig. 4(b) and Fig. 4(c). Here the simple unilateral normal contact model is used with a principal strain based evolution equation.
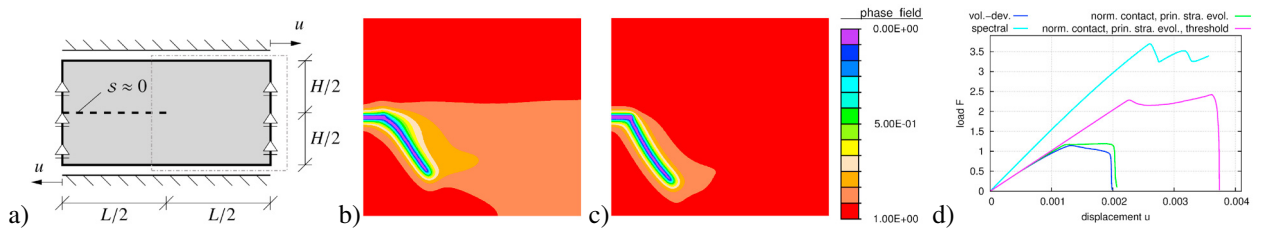
Fig. 4. Plate subjected to shear load: (a) problem setup; detail of the crack pattern of the (b) volumetric-deviatoric split, (c) simple unilateral normal contact model using a principal strain based evolution equation; (d) load deflection curves of different constitutive models.

The associated load-deflection curves are shown in Fig. 4(d). Despite similar curves, the volumetric-deviatoric split and principal strain based evolution show differences in the evolution. The introduction of a threshold value leads to a constant slope in the load-deflection curve and controls the onset of crack propagation.

6. Conclusion

The paper presented and discussed different kinds of constitutive assumptions in a generalized phase field approach to brittle fracture. This includes degradation functions as well as different types of crack evolution equations. The modeling of initial crack boundary conditions induced by the phase field indicated some difficulties of dealing with a smeared crack representation. The variational concept was given up in order to make the model more flexible. One of the proposed features is a novel non-interpenetration condition taking the crack direction into account. Its capabilities to reproduce the crack boundary condition under differend loadings were illustraded by numerical examples.

References

Ambati M., Gerasimov T., De Lorenzis L., 2014. A review on phase-field models of brittle fracture and a new fast hybrid formulation. Comput. Mech. 55(2), 383–405.

Amor H., Marigo J.-J., Maurini C., 2009. Regularized formulation of the variational brittle fracture with unilateral contact: numerical experiments. J. Mech. Phys. Solids 57, 1209–1229.

Borden M. J., Verhoosel C. V., Scott M. A., Hughes T. J. R., Landis C. M., 2012. A phase-field description of dynamic brittle fracture. Comput. Meth. Appl. Mech. Eng., 217–220, 77–95.

Bourdin B., Francfort G. A., Marigo J.-J., 2000. Numerical experiments in revisited brittle fracture. J. Mech. Phys. Solids 48, 797–826.

Bourdin B., Francfort G. A., Marigo J.-J., 2008. The variational approach to fracture. J. Elast., 91, 5–148.

Francfort G. A., Marigo J.-J., 1998. Revisiting brittle fractures as an energy minimization problem. J. Mech. Phys. Solids 46, 1319–1342.

Henry H., Levine H., 2004. Dynamic instabilities of fracture under biaxial strain using a phase field model. Phys. Rev. Lett. 93, 105504.

Hofacker M., Miehe C., 2012. Continuum phase field modeling of dynamic fracture: variational principles and staggered FE implementation. Int. J. Fract. 178, 113–129.

Karma, A., Kessler, D.A., Levine, H., 2001. Phase-field model of mode III dynamic fracture. Phys. Rev. Lett. 87, 045501.

Kuhn C., Müller R., 2010. A continuum phase field model for fracture. Eng. Fract. Mech., 77, 3625–3634.

Kuhn C., Müller R., 2013. Crack nucleation in phase field fracture models. Proc. of the 13th Int. Congress on Fracture, 1–10.

Kuhn C., Schlüter A., Müller R., 2015. On degradation functions in phase field fracture models. Comp. Mater. Sci. 108, 374–384.

Lubarda V.A., Krajcinovic D., Mastilovic S., 1994. Damage model for brittle elastic solids with unequal tensile and compressive strengths. Eng. Fract. Mech. 49, 681–697.

Miehe C., Welschinger F., Hofacker M., 2010. Thermodynamically consistent phase-field models of fracture: Variational principles and multi-field FE implementations. Int. J. Numer. Meth. Eng., 83, 1273–1311.

Miehe C., Hofacker M., Welschinger F., 2010. A phase field model for rate-independent crack propagation: Robust algorithmic implementation based on operator splits. Comput. Meth. Appl. Mech. Eng., 199(45-48), 2765–2778.

Miehe C., Schänzel L.-M., Ulmer H., 2015. Phase field modeling of fracture in multi-physics problems. Part I. Balance of crack surface and failure criteria for brittle crack propagation in thermo-elastic solids. Comput. Meth. Appl. Mech. Engrg. 294, 449–485.

Murakami S., 2012. Continuum damage mechanics: A continuum mechanics approach to the analysis of damage and fracture. Solid mechanics and its applications, 185. Springer.

Schlüter A., Willenbücher A., Kuhn C., Müller R., 2014. Phase field approximation of dynamic brittle fracture. Comput. Mech. 54, 1141–1161.

Strobl M., Seelig T., 2015. A novel treatment of crack boundary conditions in phase field models of fracture. Proc. Appl. Math. Mech. 15(1), 155–156.